Figure S1

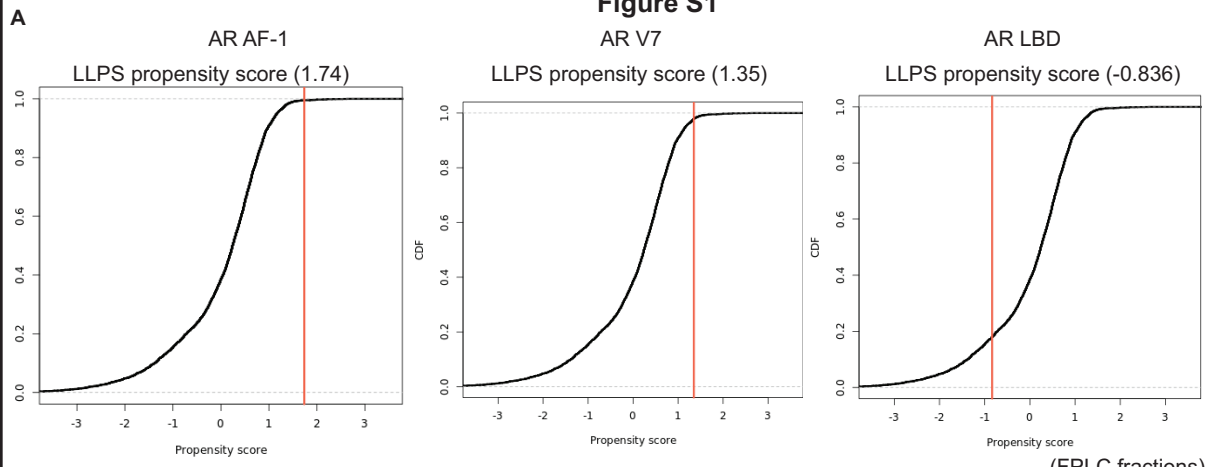
A
AR AF-1
LLPS propensity score (1.74)
AR V7
LLPS propensity score (1.35)
AR LBD
LLPS propensity score (-0.836)
CDF
Propensity score

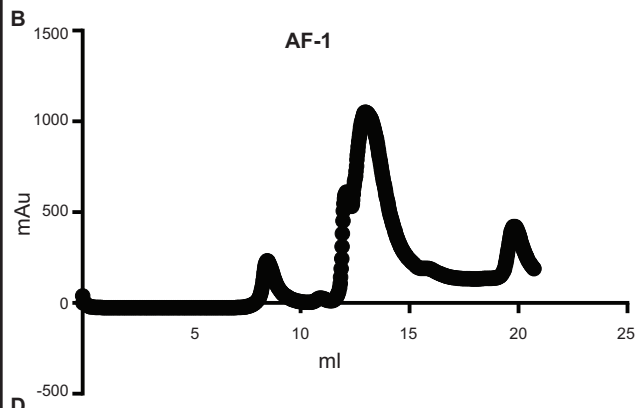
B
AF-1
mAu
ml

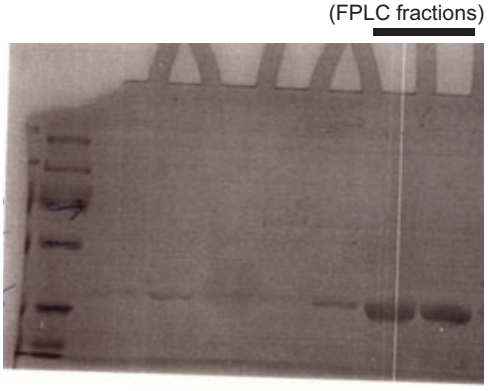
C
(FPLC fractions)

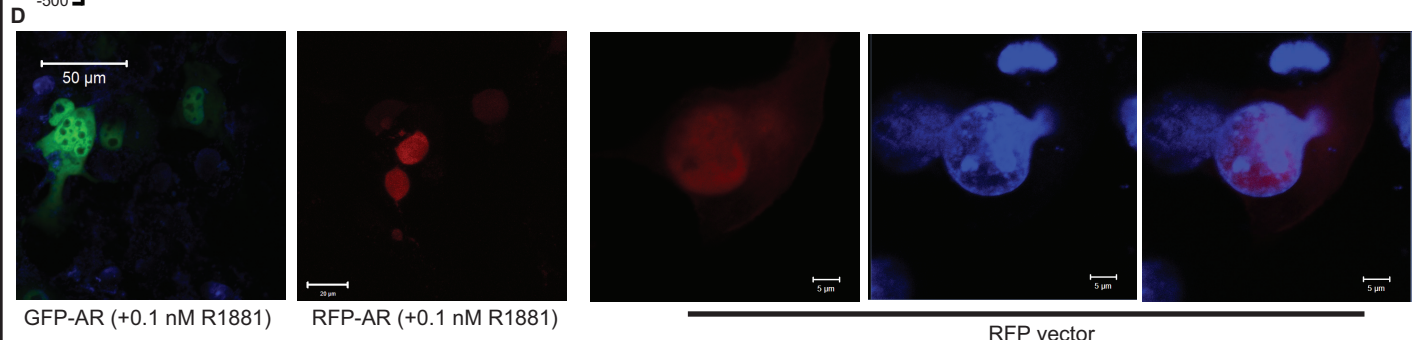
D
50 µm
GFP-AR (+0.1 nM R1881)
RFP-AR (+0.1 nM R1881)
RFP vector

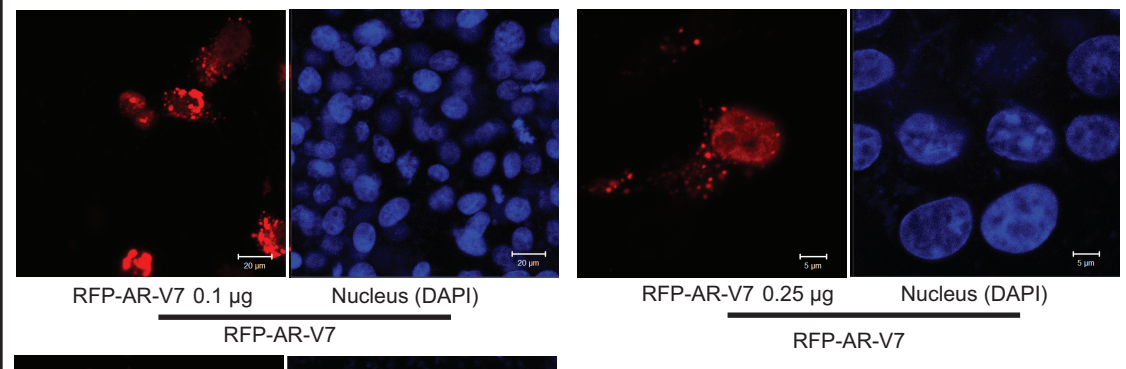
E
RFP-AR-V7 0.1 µg
Nucleus (DAPI)
RFP-AR-V7
RFP-AR-V7 0.25 µg
Nucleus (DAPI)
RFP-AR-V7

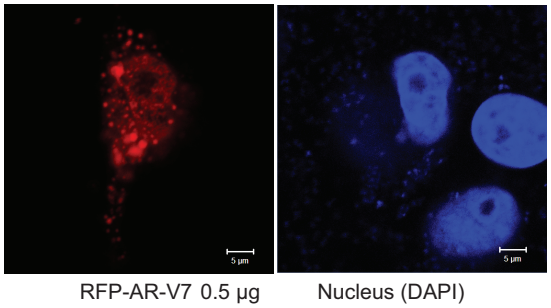
RFP-AR-V7 0.5 µg
Nucleus (DAPI)
RFP-AR-V7

Figure S2

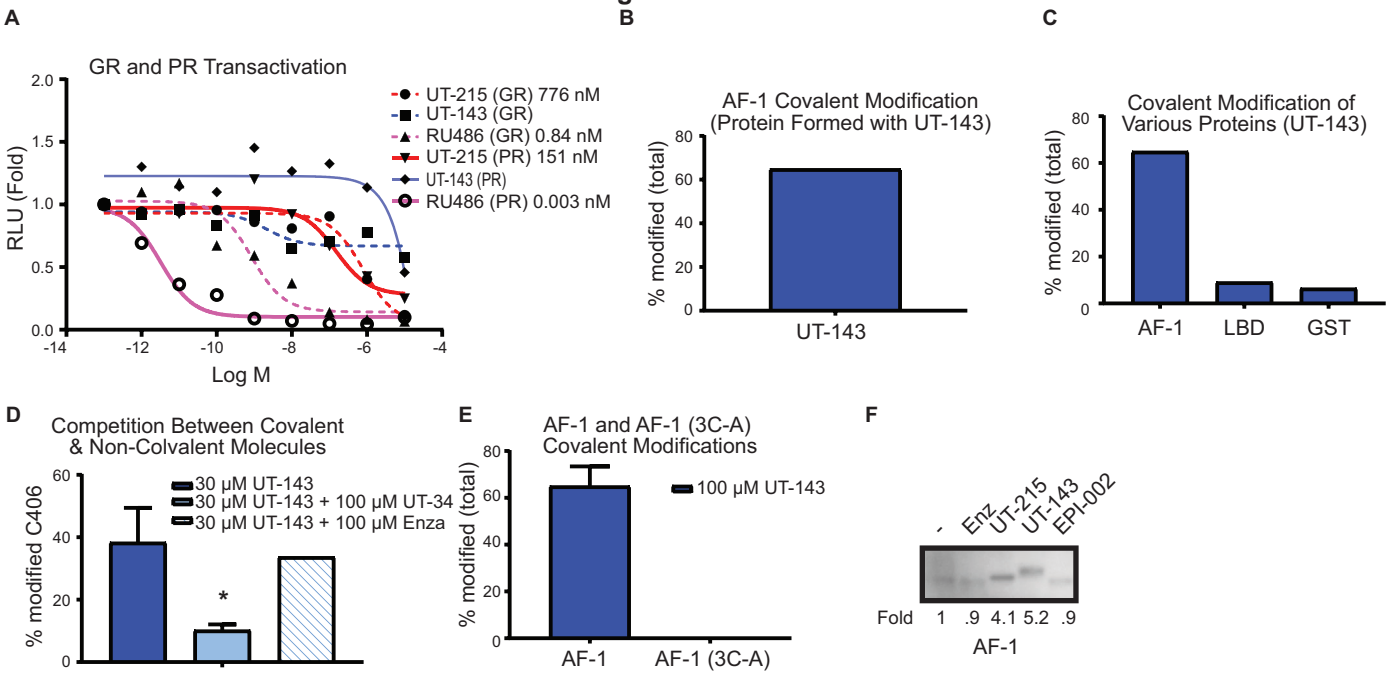
A
GR and PR Transactivation
RLU (Fold)
Log M
UT-215 (GR) 776 nM
UT-143 (GR)
RU486 (GR) 0.84 nM
UT-215 (PR) 151 nM
UT-143 (PR)
RU486 (PR) 0.003 nM
B
AF-1 Covalent Modification
(Protein Formed with UT-143)
% modified (total)
UT-143
C
Covalent Modification of
Various Proteins (UT-143)
% modified (total)
AF-1
LBD
GST
D
Competition Between Covalent
& Non-Colvalent Molecules
% modified C406
30 μM UT-143
30 μM UT-143 + 100 μM UT-34
30 μM UT-143 + 100 μM Enza
E
AF-1 and AF-1 (3C-A)
Covalent Modifications
% modified (total)
100 μM UT-143
AF-1
AF-1 (3C-A)
F
-
Enz
UT-215
UT-143
EPI-002
Fold 1 .9 4.1 5.2 .9
AF-1

Figure S3

RIME Assay pathway analysis

Vehicle unique top pathways	P-value
Spliceosome	1.18^{-21}
Ribosome	2.26^{-21}
RNA transport	5.46^{-20}
Ribosome biogenesis	5.72^{-14}

Drug unique top pathways	P-value
Spliceosome	0.0062

Common top pathways	P-value
Ribosome	8.66^{-36}
Spliceosome	1.58^{-17}
RNA transport	0.0000152
Non-homologous end-joining	0.0058

Figure S4

A

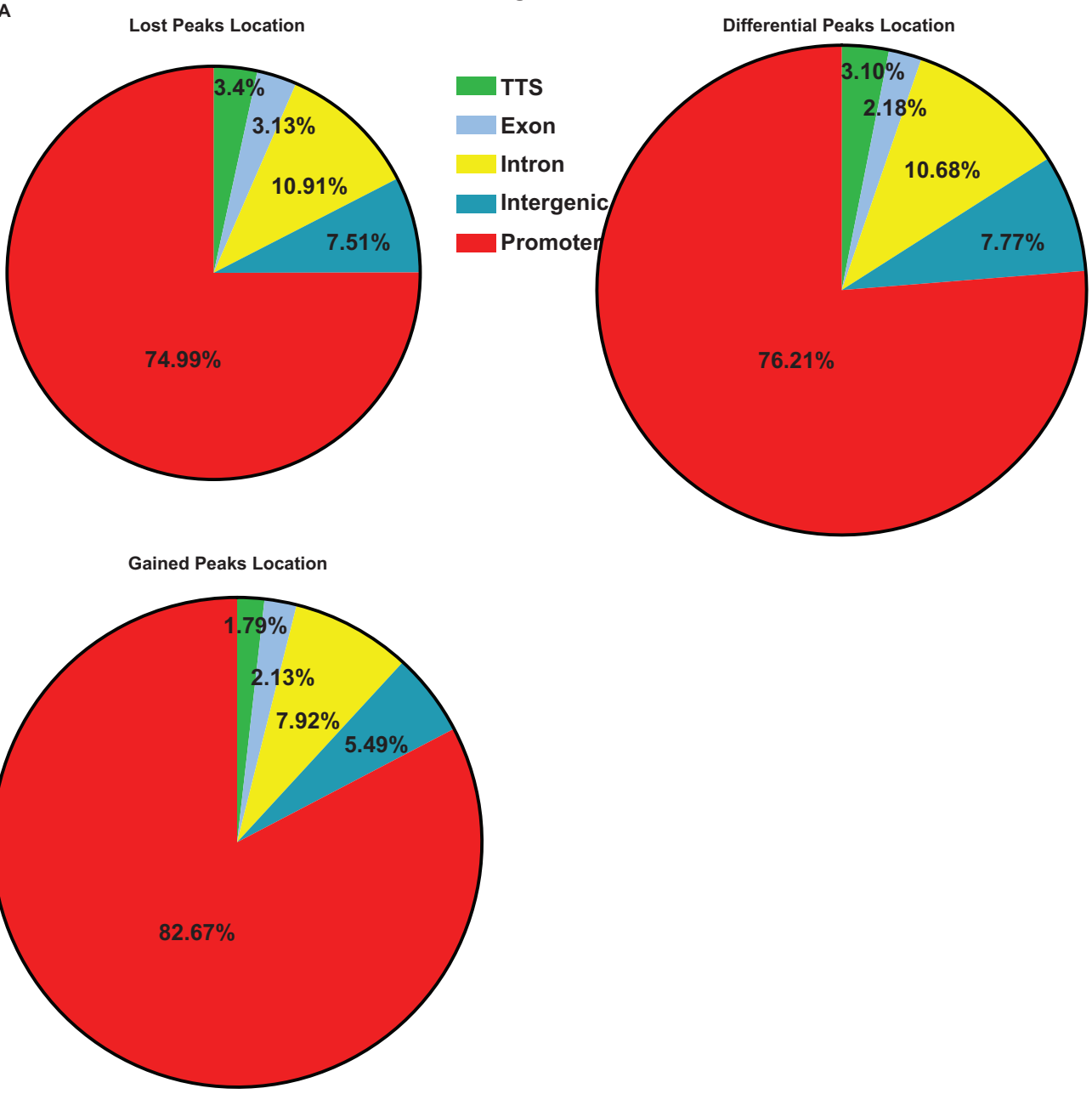

B

Drug unique top motifs	P-value	% of target
NYF (CCAAT)	1^{-1438}	35
SP2	1^{-1087}	52
GYF	1^{-293}	8
ELK1	1^{-243}	25

Vehicle unique top motifs	P-value	% of target
SP2	1^{-2372}	41
CCAAT enhancer	1^{-2035}	24
ELK4	1^{-808}	25
E2F	1^{-710}	45

Common top motifs	P-value	% of target
SOX17	1^{-4}	50
TEAD3	1^{-4}	50

Figure S4 (Cont..)

C

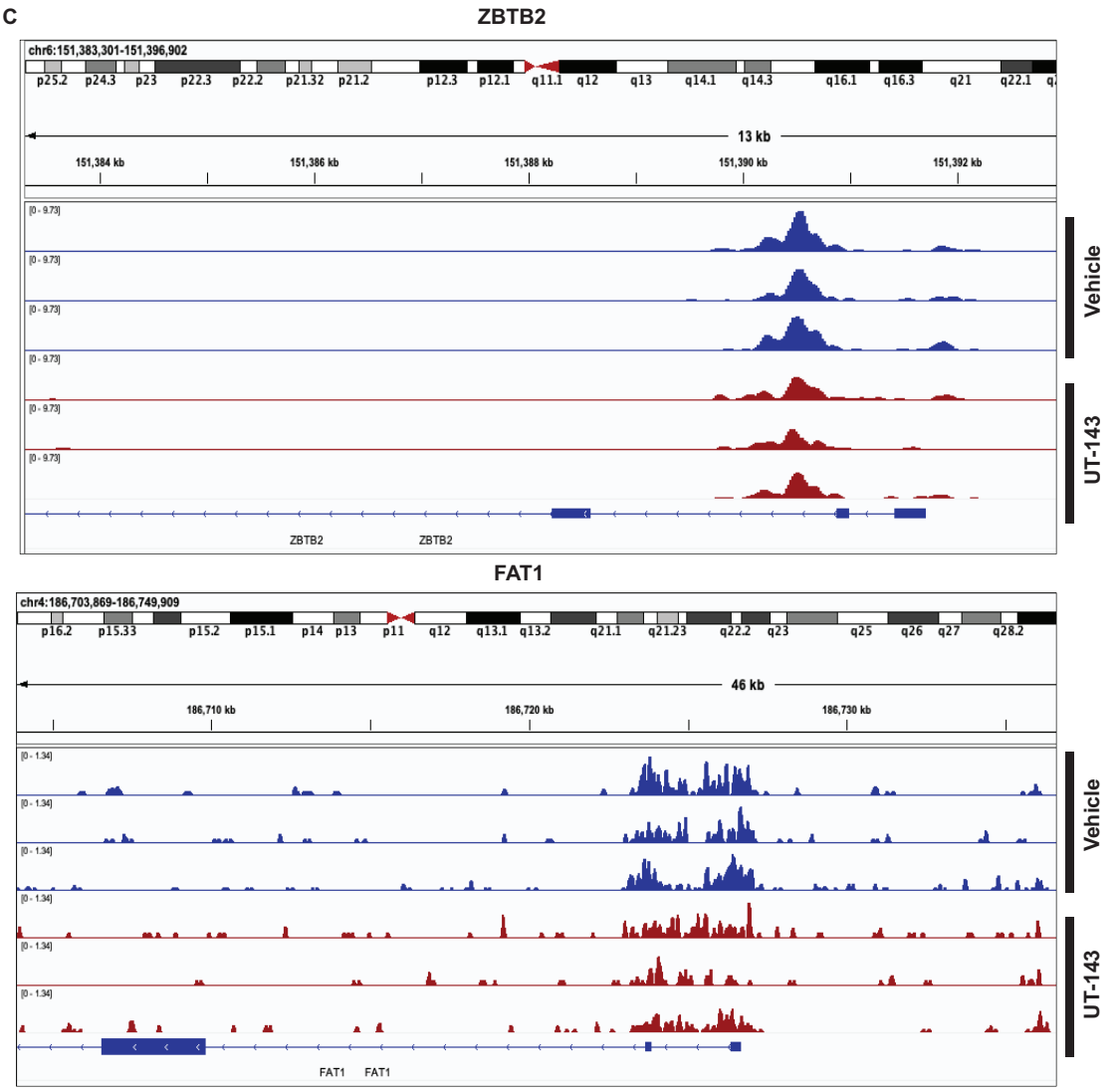

D

GO of common peaks	P-value
Biological functions	
Metabolic process	1.72^{-9}
Cellular metabolic process	1.07^{-8}
Primary metabolic process	1.83^{-8}
Cell cycle	1.07^{-7}
Molecular functions	
Organic cyclic compound binding	0.0000068
Heterocyclic compound binding	0.0000068
Enzyme binding	0.00042
RNA binding	0.0016

GO of Vehicle unique	P-value
Biological functions	
ATPase activity	3^{-32}
Active ion transmembrane	8.08^{-21}
Catalytic activity	1.03^{-16}
Active transmembrane transporter	2.82^{-16}
Molecular functions	
AP-type membrane coat adaptor complex	7.21^{-15}
cytoplasmic part	8.75^{-9}
cyclin-dependent protein kinase holoenzyme complex	7.72^{-7}
clathrin adaptor complex	1.61^{-6}

GO of Drug unique	P-value
Biological functions	
ATPase activity, coupled to movement of substances	3.5^{-9}
fatty acid derivative binding	6.85^{-7}
fatty-acyl-CoA binding	5.71^{-7}
active transmembrane transporter activity	1.39^{-6}
Molecular functions	
centriole	8.41^{-4}
plasma membrane protein complex	2.06^{-3}
cullin-RING ubiquitin ligase complex	2.12^{-3}
organelle lumen	1.7^{-3}

Figure S5

A

Group 1: 48 genes with 644 PPIs

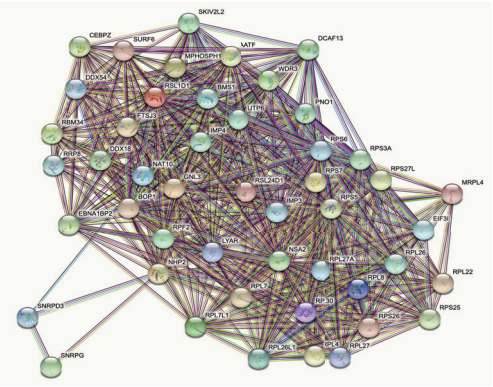

Group 1 Enriched Pathways	source	external_id	members_input_overlap	#Matched	size	p-value	q-value
Metabolism of RNA	Reactome	R-HSA-8953854	UTP6; RPS27L; RPL7; RPL27A; DCAF13; RPS6; RPS5; NHP2; SNRPD3; BMS1; RPL8; RPL27; RPL26; RPL22; RPL4; RPS26; IMP3; RPS25; WDR3; IMP4; MPHOSPH10; SNRPG; RPS7; RPL26L1; RPL30; RPS3A	11	584	3.62E-27	1.92E-25
Formation of a pool of free 40S subunits	Reactome	R-HSA-72689	RPS26; EIF3I; RPS25; RPL26L1; RPS27L; RPL27A; RPL7; RPL4; RPL26; RPL8; RPL22; RPS7; RPS6; RPS5; RPS3A; RPL30; RPL27	10	113	3.75E-26	9.94E-25
L13a-mediated translational silencing of Ceruloplasmin expression	Reactome	R-HSA-156827	RPS26; EIF3I; RPS25; RPL26L1; RPS27L; RPL27A; RPL7; RPL4; RPL26; RPL8; RPL22; RPS7; RPS6; RPS5; RPS3A; RPL30; RPL27	9	123	1.74E-25	2.14E-24
Ribosome - Homo sapiens (human)	KEGG	path:hsa03010	RPS26; RPS25; RPL26L1; RPL8; RPS27L; RPL7; RPL27A; RPL26; MRPL4; RPL30; RPL22; RPS7; RPS6; RPS5; RPS3A; RSL24D1; RPL4; RPL27	9	158	1.89E-25	2.14E-24
GTP hydrolysis and joining of the 60S ribosomal subunit	Reactome	R-HSA-72706	RPS26; EIF3I; RPS25; RPL26L1; RPS27L; RPL27A; RPL7; RPL4; RPL26; RPL8; RPL22; RPS7; RPS6; RPS5; RPS3A; RPL30; RPL27	8	124	2.01E-25	2.14E-24
Peptide chain elongation	Reactome	R-HSA-156902	RPS26; RPS25; RPL26L1; RPS27L; RPL27A; RPL7; RPL4; RPL26; RPL8; RPL22; RPS7; RPS6; RPS5; RPS3A; RPL30; RPL27	8	100	4.93E-25	3.58E-24
Cap-dependent Translation Initiation	Reactome	R-HSA-72737	RPS26; EIF3I; RPS25; RPL26L1; RPS27L; RPL27A; RPL7; RPL4; RPL26; RPL8; RPL22; RPS7; RPS6; RPS5; RPS3A; RPL30; RPL27	8	131	5.41E-25	3.58E-24
Eukaryotic Translation Initiation	Reactome	R-HSA-72613	RPS26; EIF3I; RPS25; RPL26L1; RPS27L; RPL27A; RPL7; RPL4; RPL26; RPL8; RPL22; RPS7; RPS6; RPS5; RPS3A; RPL30; RPL27	8	131	5.41E-25	3.58E-24
Eukaryotic Translation Termination	Reactome	R-HSA-72764	RPS26; RPS25; RPL26L1; RPS27L; RPL27A; RPL7; RPL4; RPL26; RPL8; RPL22; RPS7; RPS6; RPS5; RPS3A; RPL30; RPL27	7	103	8.19E-25	4.34E-24
Selenocysteine synthesis	Reactome	R-HSA-2408557	RPS26; RPS25; RPL26L1; RPS27L; RPL27A; RPL7; RPL4; RPL26; RPL8; RPL22; RPS7; RPS6; RPS5; RPS3A; RPL30; RPL27	7	103	8.19E-25	4.34E-24
independent of the Exon Junction Complex (EJC)	Reactome	R-HSA-975956	RPS26; RPS25; RPL26L1; RPS27L; RPL27A; RPL7; RPL4; RPL26; RPL8; RPL22; RPS7; RPS6; RPS5; RPS3A; RPL30; RPL27	6	105	1.14E-24	5.03E-24
Eukaryotic Translation Elongation	Reactome	R-HSA-156842	RPS26; RPS25; RPL26L1; RPS27L; RPL27A; RPL7; RPL4; RPL26; RPL8; RPL22; RPS7; RPS6; RPS5; RPS3A; RPL30; RPL27	6	105	1.14E-24	5.03E-24
Response of EIF2AK4 (GCN2) to amino acid deficiency	Reactome	R-HSA-9633012	RPS26; RPS25; RPL26L1; RPS27L; RPL27A; RPL7; RPL4; RPL26; RPL8; RPL22; RPS7; RPS6; RPS5; RPS3A; RPL30; RPL27	6	111	2.94E-24	1.20E-23
Nonsense Mediated Decay (NMD) enhanced by the Exon Junction Complex (EJC)	Reactome	R-HSA-975957	RPS26; RPS25; RPL26L1; RPL8; RPS27L; RPL7; RPL4; RPL26; RPL27A; RPL30; RPL22; RPS7; RPS6; RPS5; RPS3A; RPL27	6	117	7.18E-24	2.54E-23
Nonsense-Mediated Decay (NMD)	Reactome	R-HSA-927802	RPS26; RPS25; RPL26L1; RPL8; RPS27L; RPL7; RPL4; RPL26; RPL27A; RPL30; RPL22; RPS7; RPS6; RPS5; RPS3A; RPL27	6	117	7.18E-24	2.54E-23
SRP-dependent cotranslational protein targeting to membrane	Reactome	R-HSA-1799339	RPS26; RPS25; RPL26L1; RPS27L; RPL27A; RPL7; RPL4; RPL26; RPL8; RPL22; RPS7; RPS6; RPS5; RPS3A; RPL30; RPL27	6	123	1.67E-23	5.54E-23
Selenoamino acid metabolism	Reactome	R-HSA-2408522	RPS26; RPS25; RPL26L1; RPS27L; RPL27A; RPL7; RPL4; RPL26; RPL8; RPL22; RPS7; RPS6; RPS5; RPS3A; RPL30; RPL27	6	128	3.27E-23	1.02E-22

Group 2: 21 genes with 117 PPIs

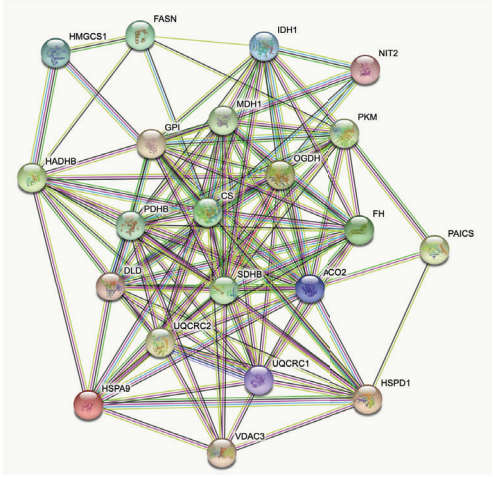

Group 2 enriched pathways	source	external_id	Matched members	#Matched	size	p-value	q-value
Warburg Effect	SMPDB	SMP00654	OGDH; SDHB; GPI; DLD; IDH1; FH; MDH1; CS; PDHB; ACO2; PKM	11	45	5.45E-23	5.94E-21
superpathway of conversion of glucose to acetyl CoA and entry into the TCA cycle	HumanCyc	PWY66-407	OGDH; SDHB; GPI; DLD; CS; MDH1; FH; PDHB; ACO2; PKM	10	48	3.38E-20	1.84E-18
Citrate cycle (TCA cycle) - Homo sapiens (human)	KEGG	path:hsa00020	OGDH; SDHB; DLD; IDH1; FH; MDH1; CS; PDHB; ACO2	9	30	1.06E-19	3.84E-18
The citric acid (TCA) cycle and respiratory electron transport	Reactome	R-HSA-1428517	OGDH; ACO2; DLD; CS; FH; PDHB; SDHB; UQCRC2; UQCRC1	9	162	1.12E-12	4.70E-12
TCA cycle	EHMN	TCA cycle	OGDH; SDHB; DLD; IDH1; CS; MDH1; FH; ACO2	8	30	4.45E-17	6.93E-16
Citrate cycle	INOH	None	OGDH; SDHB; DLD; CS; MDH1; FH; ACO2; PKM	8	32	7.99E-17	8.70E-16
Metabolic reprogramming in colon cancer	Wikipathways	WP4290	ACO2; GPI; PAICS; FASN; FH; PDHB; SDHB; PKM	8	42	8.88E-16	5.10E-15
Amino Acid metabolism	Wikipathways	WP3925	OGDH; DLD; IDH1; CS; MDH1; FH; ACO2; PKM	8	91	6.13E-13	2.78E-12
TCA cycle	HumanCyc	PWY66-398	OGDH; SDHB; DLD; FH; MDH1; CS; ACO2	7	19	3.70E-16	3.67E-15
Pyruvate metabolism and Citric Acid (TCA) cycle	Reactome	R-HSA-71406	OGDH; SDHB; DLD; CS; FH; PDHB; ACO2	7	53	1.10E-12	4.70E-12
Citric acid cycle (TCA cycle)	Reactome	R-HSA-71403	OGDH; SDHB; DLD; CS; FH; ACO2	6	22	4.89E-13	2.32E-12
TCA Cycle and Deficiency of Pyruvate Dehydrogenase complex (PDHc)	Wikipathways	WP2453	OGDH; DLD; IDH1; CS; MDH1; FH	6	16	5.28E-14	2.88E-13
TCA Cycle (aka Krebs or citric acid cycle)	Wikipathways	WP78	OGDH; SDHB; DLD; CS; FH; ACO2	6	17	8.15E-14	4.04E-13
Glycolysis and Gluconeogenesis	EHMN	Glycolysis and Gluconeogenesis	CS; PDHB; PKM; GPI; DLD	5	67	4.70E-08	1.77E-07
Pyruvate metabolism - Homo sapiens (human)	KEGG	path:hsa00620	FH; PDHB; DLD; MDH1; PKM	5	47	8.22E-09	3.20E-08
Diabetic cardiomyopathy - Homo sapiens (human)	KEGG	path:hsa05415	VDAC3; PDHB; SDHB; UQCRC2; UQCRC1	5	203	1.25E-05	3.10E-05
Protein localization	Reactome	R-HSA-9609507	CS; HSPD1; IDH1; ACO2; HSPA9	5	165	4.57E-06	1.32E-05

B

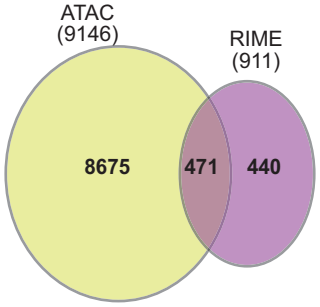

C

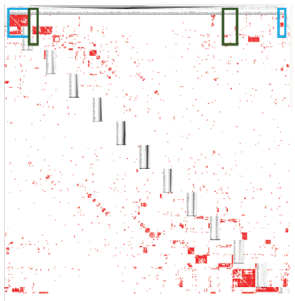

Figure S6

A

22RV1 RNA-Sequencing

GO Biological Functions	P-value
DNA replication	1.05^{-21}
DNA repair	3.07^{-15}
Spliceasomes	9.45^{-11}
Cell division	3.96^{-8}

GO Molecular Functions	P-value
DNA helicase	2.38^{-16}
ATPase activity	2.05^{-14}
Protein binding	6.83^{-13}
ATP binding	1.39^{-9}

B

22RV1 RNA-Sequencing GSEA

GO Biological Functions	P-value
Hallmark apoptosis	0.297
Hallmark p53 pathway	0.293

Figure S6 (Cont..)

C

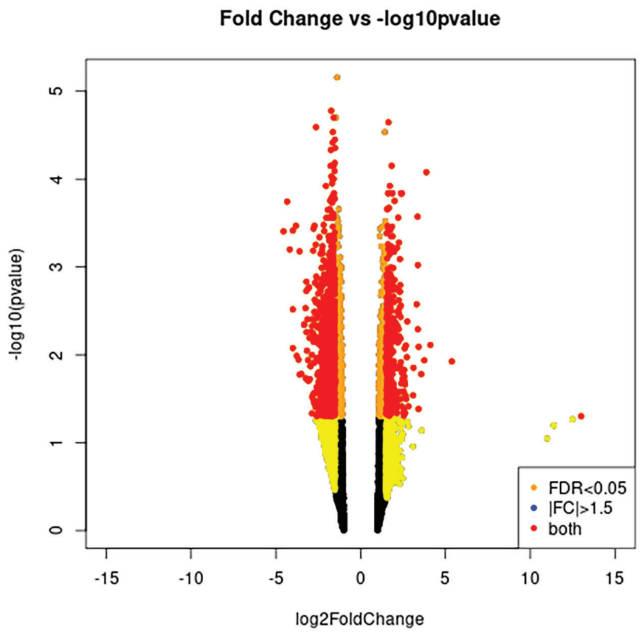

Figure S7

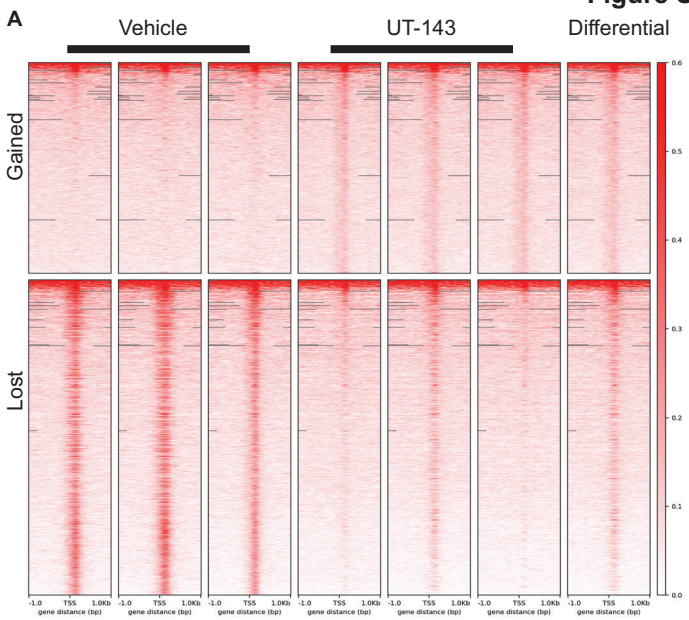
A
Vehicle
UT-143
Differential
Gained
Lost
-1.0
TSS
1.0Kb
gene distance (bp)
0.6
0.5
0.4
0.3
0.2
0.1
0.0

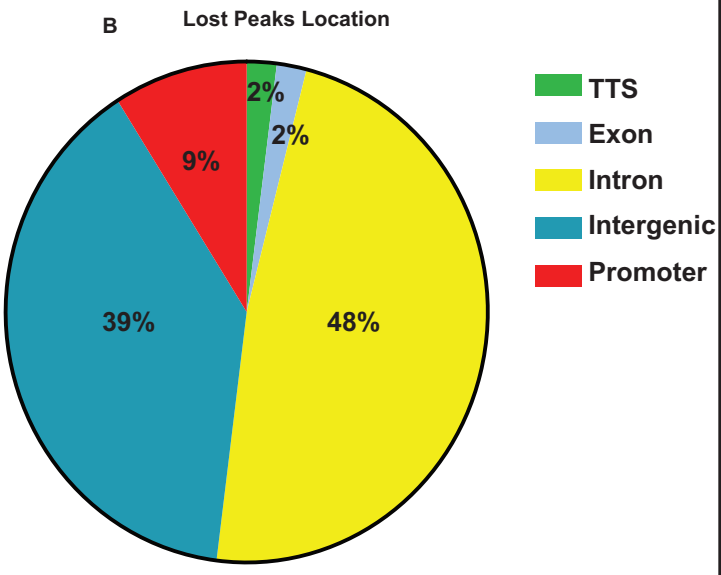
B
Lost Peaks Location
2%
2%
9%
39%
48%
TTS
Exon
Intron
Intergenic
Promoter

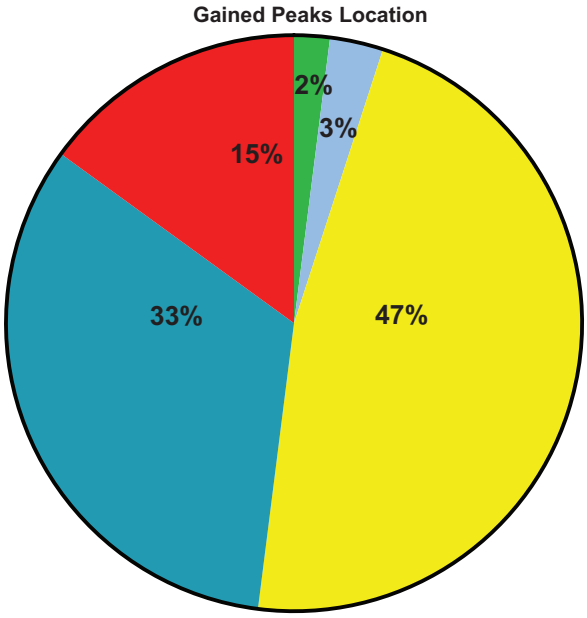
Gained Peaks Location
2%
3%
15%
33%
47%

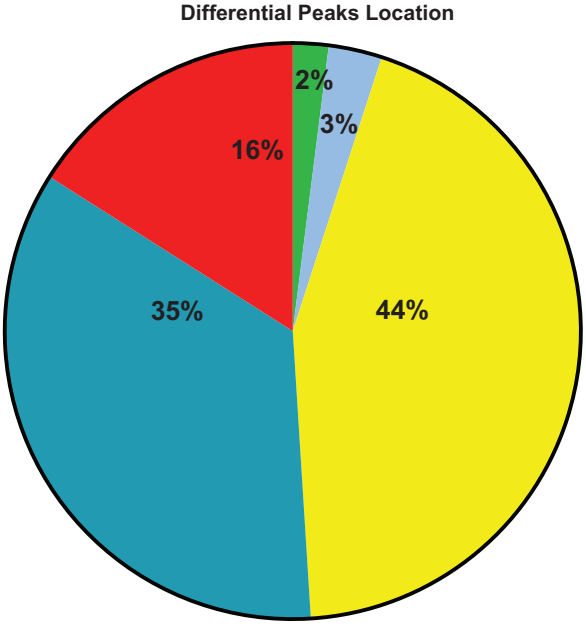
Differential Peaks Location
2%
3%
16%
35%
44%

Figure S7

C

Drug unique motifs	P-value	% of target
FOXM1	1^{-687}	18.09
CTCF	1^{-300}	3.83
Fra1	1^{-242}	5.25
NFIX	1^{-194}	26.41

Veh. unique motifs	P-value	% of target
FOXM1	1^{-2174}	31.14
PRE	1^{-845}	10.72
CTCF	1^{-690}	5.28
NF1	1^{-415}	27.91

Diff. Lost motifs	P-value	% of target
FOXM1	1^{-1284}	32.46
GRE	1^{-564}	10.34
KLF1	1^{-306}	11.88
ETV2	1^{-193}	26.81

Figure S7 (Cont..)

D

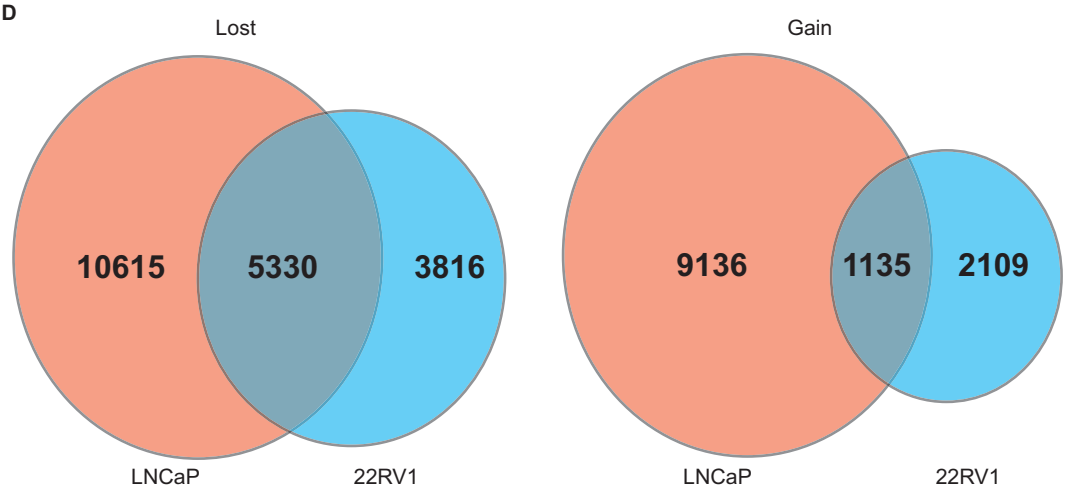

E

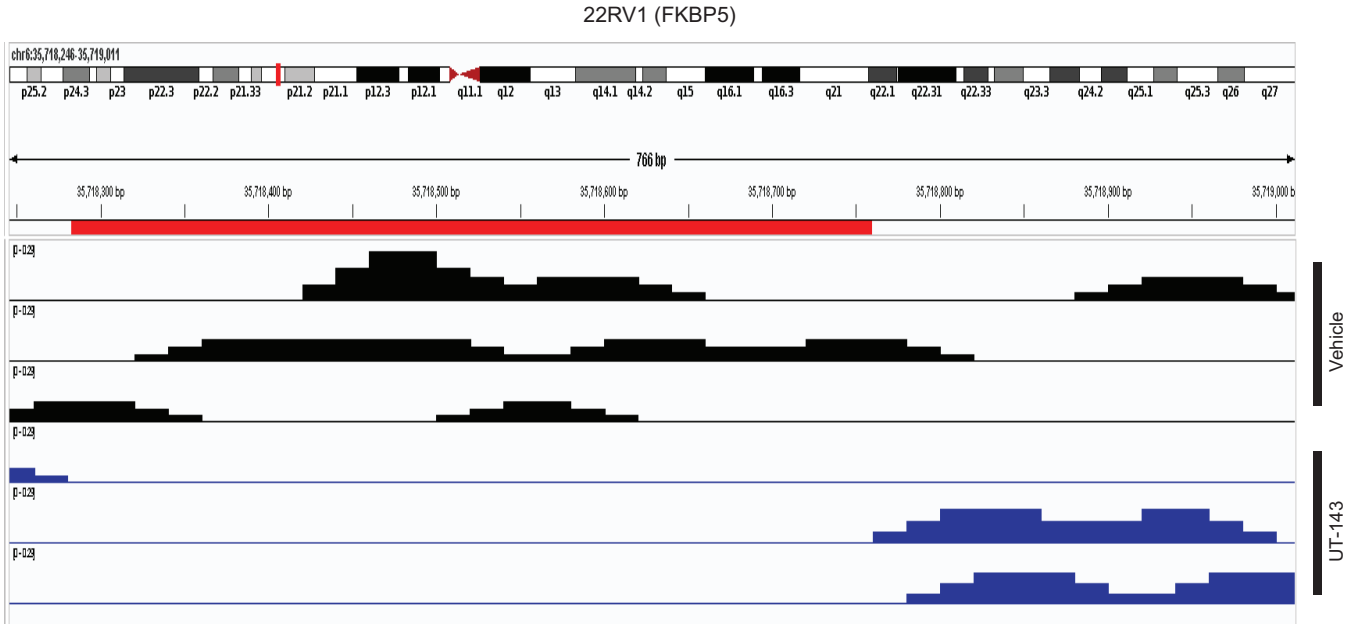

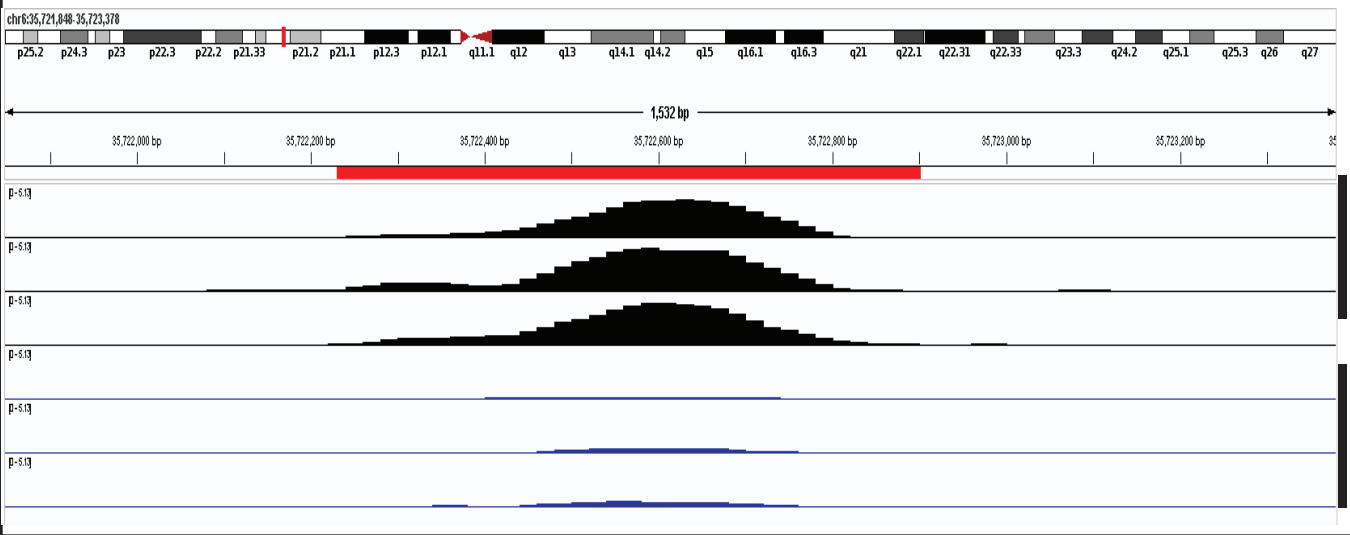

Figure S8

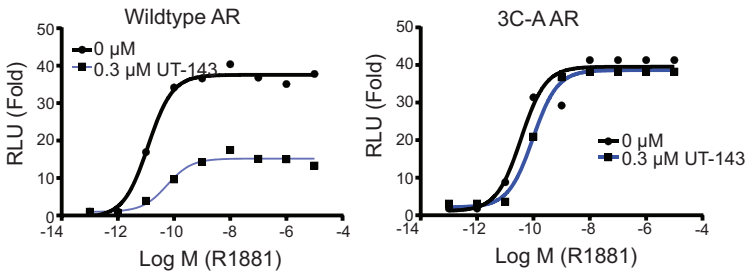
Wildtype AR
0 μM
0.3 μM UT-143
RLU (Fold)
Log M (R1881)
3C-A AR
0 μM
0.3 μM UT-143
RLU (Fold)
Log M (R1881)

Figure S9

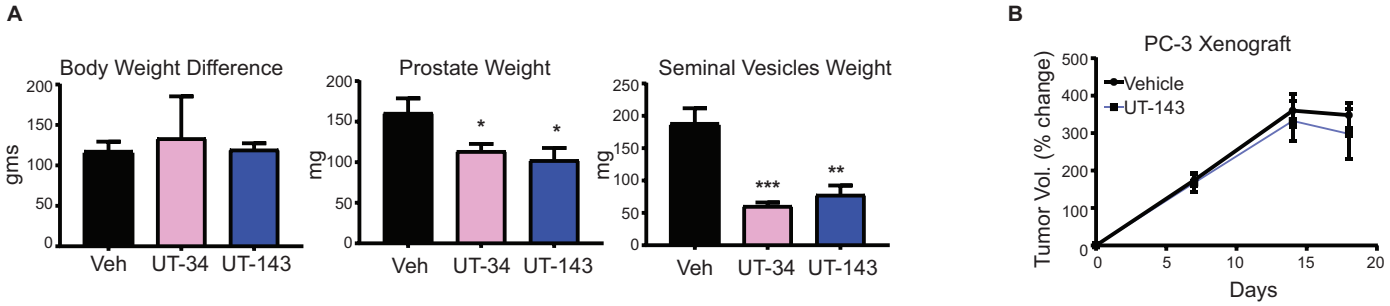
A
Body Weight Difference
gms
200
150
100
50
0
Veh
UT-34
UT-143
Prostate Weight
mg
200
150
100
50
0
*
*
Veh
UT-34
UT-143
Seminal Vesicles Weight
mg
250
200
150
100
50
0
***
**
Veh
UT-34
UT-143
B
PC-3 Xenograft
Vehicle
UT-143
Tumor Vol. (% change)
500
400
300
200
100
0
0
5
10
15
20
Days

Table ST1

Peptide	M.Wt. (-UT-215/143)	M.Wt. (+UT-215)	M.Wt. (+UT-143)
C327 GLEGESLG**C**SGSAAAGSSGTLELPSTLSLYK	2942.43	3280.51	3404.56
C406 LENPLDYGSAWAAAAAQ**C**R	2008.95	2347.02	2471.07
C267 GD**C**MYAPLLGVPPAVRPTPCAPLAECK	2769.36	3107.43	3231.48
C240 DNYLGGTSTISDNAKELCK	2028.95	No modifications	
C284 GD**C**MYAPLLGVPPAVRPTP**C**APLAECK	2769.36		
C290 GD**C**MYAPLLGVPPAVRPTPCAPLAE**C**K	2769.36		

Table ST2

Reagent	Source	Cat. No. (if applicable)
Lipofectamine	Thermofisher	18324020
Cell culture medium	Corning	10-040-CV
Fetal bovine serum (FBS)	Atlanta Biologicals	S11150H
Charcoal-stripped FBS	GE	SH3006803
Dual-luciferase kit	GoldBio	I-920-1000
Cells-to-ct kit	Thermofisher	4399003
Enzalutamide	Medkoo Biosciences	201821
RU486	Sigma	475838-50MG
EPI-002	MedChem Express	HY-109070
AR antibody PG21	Millipore	352054
GAPDH antibody	Millipore	G9545-100UL
TaqMan probes	Thermofisher	
^{3}H R1881	Perkin Elmer	NET590250UC
GST resin	GoldBio	G-250-10
IPTG	GoldBio	I2481C25
Glutathione	GoldBio	G155-25
IP magnetic beads	Millipore	LSKMAGAG02
Precision protease	GE	45 001 319
Superdex column	GE	
Purified AR protein	Sigma	SRP2161
Cell line authentication	Genetica	
AR-V7 antibody	RevmAb	31-110900
AR C-19 antibody	Abcam	ab52615
AR LBD purified protein for IP	Protein Tech	Ag17385
AR ChIP antibody	Cell signaling	5153S

Supplement Figure Legends

Figure S1. A. catGRANULE LLPS formation score. Sequence belonging to various proteins indicated in the panel was loaded onto the catGRANULE website and the LLPS formation score was obtained. **B. FPLC profile**. AF-1 purified using GST resin was concentrated and loaded on a FPLC attached to Superdex size-exclusion column. FPLC profile is shown. **C. Purified FPLC fractions**. FPLC fractions 12-14 were concentrated and loaded on an SDS-PAGE and the proteins were stained with Coomassie blue. **D**. Fluorescent tagged AR or vector plasmid was transfected into COS7 cells. Confocal microscopy was performed 48 hours after transfection. Live or fixed cells were used for imaging. Fixed cells were counter-stained with DAPI. **E**. A dose response of RFP-AR-V7 transfection was performed and AR-V7 was imaged using a confocal microscope.

Figure S2: A. GR and PR transactivation. Transactivation assay was performed in COS7 cells transfected with GRE-LUC, GR or PR, and CMV-renilla-LUC. Cells in DME+5% csFBS w/o phenol red were treated with 0.1 nM dexamethasone or 1 nM progesterone in the presence of covalent compounds, or RU486, and luciferase assay was performed 24 hours after treatment. **B**. **UT-143 covalently binds to AF-1 in vivo**. UT-143 (30 μM) was added to the bacterial culture when AF-1 protein synthesis was induced with 1 mM IPTG. Cells were harvested, protein purified, and mass spectrometry experiment was performed. % Modified peptides is indicated as bar graph. **C. Cross-reactivity of covalent binding**. Purified recombinant AR AF-1, LBD, or GST protein (10 μg) was incubated in the presence of 100 μM SARICA for 12-16 hours at 4°C. Protein was digested with trypsin overnight at 4°C and the peptides were identified by mass spectrometer. Modified peptide was quantified and represented as percent modified peptides (representative of n=3-5). **D. UT-34 competes for the binding region with UT-143**. Mass Spectrometry experiment

was performed by pre-incubating with 100 μM UT-34 or enzalutamide for 2 hours at 4°C, followed by 30 μM UT-143 overnight at 4°C. Trypsin-digested peptides were profiled using a mass spectrometer. Percent of modified C406 is represented (n=3-5). Enzalutamide was used as a negative control. **E. Mutation of C267, C327, and C406 blocks covalent binding of UT-143 to AF-1**. Mass Spectrometry experiment was performed with purified AR AF-1 and AR AF-1 with three cysteines mutated to alanines (3C-A) protein in the presence of 100 μM UT-143 (n=3). **F**. **SARICAs stabilize AF-1 protein**. Recombinant purified AF-1 protein (5 ng) was incubated at room temperature for 4 hours with DMSO or 50 μM of the indicated compounds. Proteins were fractionated on an SDS-PAGE and Western blot was performed with AR antibody (AR-441) that binds to the AF-1 region. The blots were quantified and expressed as fold change from vehicle controls. Percent modified peptides is provided as a graph. GR – glucocorticoid receptor; PR – progesterone receptor.

Figure S3. **Pathway analysis of RIME data**.

Figure S4. 22RV1 ATAC-seq data. A. Location of peaks on the DNA. B. motif analysis. C. Genome browser tracks. D. Pathway analysis.

Figure S5. A. 22RV1 RIME-ATAC common gene set and protein-protein interaction nodules. **B and C. Venn diagram of 22RV1 RIME and ATAC-seq.**

Figure S6. 22RV1 RNA-sequencing pathway map (A), GSEA analysis (B), and volcano plot (C).

Figure S7. ATAC-Seq in LNCaP cells. LNCaP cells maintained in RPMI+10% FBS were treated with vehicle or 10 μM UT-143 for 16-20 hours (n=3/group). Cells were harvested and ATAC-seq was performed. Heatmap (**A)**, peak distribution in the genome (**B**), and GO pathway analysis (**C**) are shown. LNCaP and 22RV1 ATAC-seq annotated peaks for lost and gain regions are shown as Venn diagram (**D**). **E**. IGV tracks of FKBP5 regulatory regions in LNCaP and 22RV1 ATAC-seq are shown.

Figure S8. UT-143 irreversibly inhibits AR but not AR 3C-A. COS7 cells were transfected with wildtype AR or AR with 3 cysteines mutated to alanines. Cells in DME+5% csFBS w/o phenol red were treated with a dose-response (1 pM to 10 μM) of R1881 in the presence or absence of 0.3 μM UT-143. Dual luciferase assay was performed 24 hours after treatment (n=3).

Figure S9. A. UT-143 is comparable to UT-34 in reducing prostate and seminal vesicles. Male Sprague Dawley rats (n=5/group) were treated orally with vehicle (20% DMSO + 80% PEG-300), 20 mg/kg UT-34 or UT-143 for 13 days. Body weight was recorded at study initiation and at sacrifice. Animals were sacrificed on day 14, and prostate and seminal vesicles were weighed. **B. UT-143 does not affect AR-negative PC-3 tumor xenograft growth**. PC-3 cells were implanted subcutaneously in male NSG mice. Once the tumors grow to 100-300 mm^3, the animals were randomized and treated orally with vehicle (DMSO:PEG-300) or 60 mg/kg/day UT-143 (n=5/group). Tumor volume was measured twice weekly.

Table ST1. Peptides that were detected by mass spectrometer and modified by SARICAs.

Table ST2. Materials information.

Supplement Methods

Rapid immunoprecipitation mass spectrometry of endogenous protein (RIME) assay. RIME assay was performed as published before with modifications of previous publications[1, 2]. The cells were fixed with 1% methanol-free formaldehyde at room temperature for 20 min. The cells were washed in ice cold 1XPBS and were scraped in PBS containing protease and phosphatase inhibitors and 5 mM sodium butyrate. The cells were centrifuged at 7000 rpm for 5 minutes and lysed in 375 µl lysis buffer (10mM Tris pH8.1, 10 mM EDTA, 1% SDS with 1x PIC, PMSF, 5 mM sodium butyrate) on ice for 30 minutes. The cell lysates were sonicated with a probe -sonicator (10 cycles – 10 pulse and 20 sec intervals). Cell debris were pelleted, and the supernatant transferred to a new tube.

Dyna A/G magnetic beads (25 µl each) were prepared by washing three times with 500 µl of 1x PBS plus 0.5% BSA. The beads were reconstituted in fresh PBS with 0.5 % BSA and incubated on a rotator at 4°C for 6 hours with AR-V7 antibody (1.5 µl from RevMab Cat #31-110900) or IgG. The unbound antibody was washed with PBS BSA solution twice. Protein (1 mg/ml) was made up in ChIP dilution buffer (1% Triton X-100, 2 mM EDTA, 150 mM NaCl, 20 mM Tris pH 8.1 + 1x PIC + 5 mM Sodium Butyrate) and incubated with the antibody-bound meads overnight at 4°C on a rotor. The magnetic beads were washed with 1 mL of cold RIPA + .3 M NaCl buffer once. The beads were washed with ice cold RIPA buffer once and with 100 mM ammonium bicarbonate buffer four times. The beads were submitted for mass spectrometry as described in the supplement methods.

Quantitative proteomics data was analyzed by the Molecular Bioinformatics core at UTHSC. Data was log_2 transformed and normalized using a Loess cyclic normalization limma package in R[3]. The mean, median, standard deviation, and coefficient of variance were calculated for every protein measured. Principle component analysis and Pearson's coefficient plots were performed on the normalized proteome profile. The mean score of the IgG control samples was subtracted from the mean score of the AR-V7 antibody samples to remove background expression. After noise was removed, the two sample groups were compared to determine the proteins that were differentially regulated between experimental conditions. Differential proteins were identified by calculated fold change, and a Wilcoxon's t test was used to determine significance between conditions. All proteins that fail to yield a p value less than 0.05 were removed. Benjamini - Hochberg false discovery rate was performed on the trimmed gene list[4]. All proteins that fail to yield a false discovery rate of less than 0.05 were removed from further analysis. Heatmaps were generated using heatmap2 in R. Differential proteomics lists were uploaded to string-db.org in order to create PPI networks and obtain pathway and gene otology analysis[5].

ATAC-Seq. ATAC-seq in triplicates was performed following the Omni-ATAC protocol as previously described[6]. Briefly, nuclei were isolated from approximately 50,000 cells in lysis buffer containing 0.1% NP-40 and 0.01% Digitonin, and were fragmented with Nextera Tn5 Transposase (TDE1, Illumina) in TD Tagment DNA buffer (Illumina) for 30 minutes at 37 °C and resulting library fragments were purified using a Qiagen MinElute kit. Libraries were amplified by 4–6 additional PCR cycles [6] and purified using AMPure XP beads (Beckman Coulter). The libraries were sequenced 2 x 75 bp on an Illumina chip to obtain at least 50 million high quality mapping reads per sample.

Quality assurance was performed using FASTQC. All reads were trimmed to remove any nucleotide that fails a phred score < Q20. The trimmed FASTQ files were aligned to the hg38 reference library using bowtie2. Once aligned, the SAM files were collected and trimmed to contain only aligned reads using SAMtools. The new sams were converted to BAM files using SAMTools. Bigwig files were generated using bamcoverage from deepTools. Bigwig files were loaded to IGV for visualization. Homer was used for peak calling and annotation using default settings and FDR < 0.1. DeepTools was used to create a list of differential peaks between conditions using default settings. Heatmaps and Venn diagrams were created in R.

Sequencing. Individual libraries from ATAC experiments, were examined using a High Sensitivity DNA chip on an Agilent Bioanalyzer and quantified by fluorescent dye binding (Q-bit). The sizes of the libraries from the Bioanalyzer and the quantity from the Q-bit were then used to calculate the molar concentration of the individual libraries. The libraries were then pooled in equimolar amounts and final quantification of the pools performed by qPCR utilizing a Takara library Quantification Kit with their standards for comparison.

The pooled libraries were then sequenced according to the manufacturer's instructions on an Illumina NextSeq 500 (2X75bases), High Output chip for the ATAC libraries.

RNA sequencing. 22RV1 cells were plated in 60 mm dishes (n=3/group) at 2 million cells/dish in RPMI+10% FBS. Cells were maintained in this medium for 2 days and were treated with vehicle or 10 μM UT-143 for 16-20 hours. Cells were harvested and RNA extracted using Qiagen RNA

purification kit. RNA with RNA integrity number (RIN) greater than or equal to 8 was given to UTHSC molecular resource (MRC) core for sequencing.

Competitive ligand-binding assay. Competitive ligand-binding assay with GST-tagged AR-LBD and 6 nM ^{3}H- R1881 was performed as described previously [7, 8]. GST-AR-LBD cloned in pGEX-4t1 was used to obtain GST-tagged LBD protein. The protein crude extract was incubated with 6 nM ^{3}H- R1881, a dose response of SARICAs (1 pM to 100 μM) or DHT (used as control in all experiments) for 16 hours at 4°C. The protein complex was precipitated using hydroxyapatite (Bio-Rad, Hercules, CA), washed 4-6 times, and the bound radioactivity was eluted using 100% ethanol. The eluted tritium was counted using a scintillation counter. The inhibitory constant (Ki) was obtained from modeling the data using SigmaPlot software.

Protein ID and Mapping of Modifications by Agents

LC-MS-MS-60min Gradient

Sample amount per injection: 0.1ug of digested protein

HPLC: Ultimate 3000RSLCnano, Thermo Fisher

Column: Acclaim PepMap RSLC, 75μm x 500mm (ID x Length), C-18, 2μm, 100Å, Thermo Fisher

Trap column: Acclaim PepMap 100, 75μm x 20mm, C18, 3μm, 100Å, Thermo Fisher

Solvent A: 0.1% formic acid in water, LC/MS grade, Thermo Fisher

Solvent B: 0.1% formic acid in acetonitrile, LC/MS grade, Thermo Fisher

Flow rate: 300nl/min

Column temperature: 40 °C

Injection volume/mode: 5µl/µlPickUp

LC Gradient: 0min-3%B, 4min-3%B, 5min-5%B, 55min-25%B, 60min-30%B, 63min-90%B, 73min-90%B,

76min-3%B, 100min-3%B

MS: Orbitrap Fusion Lumos, Thermo Fisher

Data dependent analysis (DDA): 3sec cycles

MS scan (full): Analyzer - Orbitrap, resolution-120,000 (FWHM, at m/z=200)

Scan Filters: MIPS mode - Peptide

Intensity ≥ 10,000

Charge state - 2-6

Dynamic exclusion - 30sec

MS2 scan (full): Quadrupole isolation window - 0.7m/z,

Activation - HCD (30%)

Analyzer - Ion Trap, Rapid scan

Post-Acquisition Analysis

Proteome Discoverer 2.2, Thermo Fisher

Peptide/protein identification

Search engine: Sequest HT

Database: SwissProt, TaxID 9606 (Homo sapiens), v.2017-10-25, 42252 entries

Enzyme: Trypsin (full)

Dynamic modification: Oxidation of Met

Modification of Cys and/or Lys with agent 34, 215, or 239

Precursor and fragment ion mass tolerance: 10ppm and 0.6Da, respectively

Validation and filtering of PSM (q value): Percolator, FDR ≤0.01

Validation and filtering of peptide sequence (q value): Qvality algorithm, FDR ≤0.01

Identification of protein or protein group: At least one validated peptide sequence unique to a protein or a protein group

Protein groups: Strict parsimony principle applied

Validation of protein ID: Qvality algorithm, strict - FDR≤0.01, relaxed - FDR≤0.05

Feature Detection

Min Trace Length: 5

Min # Isotopes: 2

Max ΔRT of Isotope Pattern: 0.2min

Peptide Abundance: MS Peak Area

Protein-Protein Interaction (PPI) - IP Complex – Label Free Quantification (LFQ)

LC-MS-MS-100min Gradient

HPLC: Ultimate 3000RSLCnano, Thermo Fisher

Column: Acclaim PepMap RSLC, 75µm x 500mm (ID x Length), C-18, 2µm, 100Å, Thermo Fisher

Trap column: Acclaim PepMap 100, 75µm x 20mm, C18, 3µm, 100Å, Thermo Fisher

Solvent A: 0.1% formic acid in water, LC/MS grade, Thermo Fisher

Solvent B: 0.1% formic acid in acetonitrile, LC/MS grade, Thermo Fisher

Flow rate: 300nl/min

Column temperature: 40 °C

Injection volume/mode: 5µl/µl PickUp

Gradient: 0min-3%B, 4min-3%B, 5min-5%B, 55min-25%B, 60min-30%B, 63min-90%B, 73min-90%B,

76min-3%B, 100min-3%B

MS: Orbitrap Fusion Lumos, Thermo Fisher

Data dependent analysis (DDA): 3sec cycles

MS scan (full): Analyzer - Orbitrap, resolution-120,000 (FWHM, at m/z=200)

Scan Filters: MIPS mode - Peptide

Intensity threshold ≥ 10,000

Charge state - 2-6

Dynamic exclusion - 30sec

MS2 scan (full): Quadrupole isolation window - 0.7m/z,

Activation - HCD (30%)

Analyzer - Orbitrap, Resolution 30,000 (FWHM, at m/z=200)

Post-Acquisition Analysis

Proteome Discoverer 2.4, Thermo Fisher

Peptide/Protein Identification

Search engine: Sequest HT

Target Database: SwissProt, TaxID 9606 (Homo sapiens), v.2017-05-10, 42153 entries

Decoy Database: Reversed target database

Enzyme: Trypsin (full)

Dynamic modification: Oxidation of Met, acetylation of the protein N-terminus

Static modification: Carbamidomethylation of Cys

Precursor and fragment ion mass tolerance: 10ppm and 0.02Da, respectively

Validation and filtering of PSM (q value): Percolator, FDR ≤0.01

Validation and filtering of peptide sequences (q value): Qvality algorithm, FDR ≤0.01

Identification of protein or protein group: At least one validated peptide sequence unique to a protein or a protein group

Protein grouping: Strict parsimony principle applied

Validation of protein ID (q value): strict - FDR≤0.01, relaxed - FDR≤0.05

Feature Detection

Min Trace Length: 5

Min # Isotopes: 2

Max ΔRT of Isotope Pattern Multiplets: 0.2min

Chromatographic Alignment

Max RT shift: 5min

Mass tolerance: 10ppm

Feature Linking/Mapping

RT tolerance: 0 (automatic)

Mass tolerance: 0 (automatic)

Min S/N threshold: 5

Peptide/Protein Quantification:

Quantification: LFQ - Label-free Quantification (Precursor Ion Area Detection)

Peptides to use: Unique + Razor

Peptide uniqueness: Protein Group

Peptide Abundance: LC Peak Area

Normalization mode: Total Peptide Amount

Protein abundance: Summed abundances of assigned peptides

Peptide Group abundance: Mean of bio-replicate abundances

Protein Group abundance: Mean of bio-replicate abundances

Ratio calculation: Based on summed abundances

Hypothesis test: t Test (Individual Proteins)

Adjusted p-value: Benjamini-Hochberg method

Identification of the members of a multi-protein complex specific to the protein of interest

Analytical approach: A multi-protein complex (MPC) associated with a protein of interest was isolated/separated from other components of cell lysate by immuno-precipitation (IP) using antibody specific to the protein of interest and bound to magnetic beads (reference/description of the used procedure). Isolated IP proteins comprise MPC of interest as well as background lysate proteins non-specifically bound to the beads. The background proteins (i.e., proteins other than MPC specific proteins) were determined in parallel control analysis, where the antibody was omitted (or replaced with isotype IgG). The sample proteins were identified, quantified, and the

relative abundance (molar ratio, experiment vs control) was determined for each identified/quantified protein. For statistical validation of results, four bio-replicates were included per experimental group and corresponding control group of samples. The relative abundance of each MPC specific protein (in contrast to the background proteins) was expected to significantly exceed 1; such proteins were selected as candidate MPC specific proteins (see/refer to the applied selection criteria, described by Daniel Johnson).

Sample Processing: samples (beads with bound proteins) were transferred into 100ul of digestion buffer (100mM TEAB, pH 8.3) for processing. The estimated amount of protein per experimental sample was 2ug. Sample proteins were reduced with 5mM DTT for 45 min at 50°C, alkylated with 25mM iodoacetamide for 20min at RT in dark, incubated with 25mm DTT at RT for 15min, and digested with 0.3ug of Pierce trypsin/Lys-C protease mixture (A41007, Thermo Fisher) overnight at 30°C shaking at 1100rpm. The collected peptide samples (separated from the beads) were desalted using Pierce C-18 spin tips (84850, Thermo Fisher) according to the manufacturer's protocol, and vacuum dried.

LC-MS/MS: each dried peptide sample was re-dissolved in 100ul of loading buffer (3% acetonitrile, 0.05% TFA), and 5ul was analyzed using LC-MS-MS method with 100min LC gradient for peptide/protein identification and label-free quantification (LFQ). Raw MS data were acquired on an Orbitrap Fusion Lumos mass spectrometer (Thermo Fisher) operating in line with Ultimate 3000RSLCnano UHPLS system (Thermo Fisher). The peptides were trapped on an Acclaim PepMap 100 nanoViper column (75µm x 20mm, Thermo Fisher) at 5ul/min flow rate. The trapped peptides were separated on an Acclaim PepMap RSLC nanoViper column (75µm x 500mm, C-18, 2µm, 100Å, Thermo Fisher) at 300nl/min flow rate and 40 °C column temperature using water and acetonitrile with 0.1% formic acid as solvents A and B, respectively. The

following multi-point linear gradient was applied: 3%B at 0-4min, 5%B at 5min, 25%B at 55min, 30%B at 60min, 90%B at 63-73min, and 3%B at 76-100min. Data dependent acquisition (DDA) method was used with 3sec cycles and the following MS scan parameters. Full MS scans were performed in the Orbitrap analyzer at 120,000 (FWHM, at m/z=200) resolving power to determine the accurate masses (m/z) of peptides. The following data dependent MS2 analysis was performed on precursor ions with peptide-specific isotopic pattern, charge state 2-6, and intensity of at least 10,000. For MS2 scans, peptide ions were isolated using quadrupole isolation with 0.7 m/z window, fragmented (HCD, 30% NCE), and the fragment masses were determined in the Orbitrap analyzer at 30,000 (FWHM, at m/z=200) resolving power. Dynamic exclusion was applied for 30sec.

Post-acquisition analysis of raw MS data. The analysis the acquired raw MS data was performed within a mass informatics platform Proteome Discoverer 2.4 (Thermo Fisher) using Sequest HT search algorithm and human protein database (SwissProt, Homo sapiens, TaxID 9606, v.2017-10-25, 42252 entries). The reversed target database was used as decoy database. Full tryptic peptides were searched; 2 miss-cleavages were allowed. The searched fixed modifications included: carbamidomethylation of Cys. The variable modifications included oxidation of Met and acetylation of the protein N-terminus. The precursor and fragment ion mass tolerances were set to 10ppm and 0.02Da, respectively. The raw data were filtered for the precursor ions with S/N of at least 1.5. The PSMs were filtered for further analysis using a delta Cn threshold of 0.05. The q-values were calculated at PSM level (Percolator), and then, at peptide level (Qvality algorithm) to control false discovery rate (FDR). The FDR threshold of 0.01 was used to validate and filter the data at PSMs and then at peptide levels. The validated/filtered peptides were used for the identification of the candidate precursor proteins. The following parameters were used for feature

detection, chromatographic alignment, and feature linking: 5 for minimal trace length, 10ppm for mass tolerance, automatic for RT tolerance, 5 for minimal S/N threshold. Peptide quantification was based on LC peak area with at least 5 data-points. Protein abundances were determined as summed abundances of assigned peptides. Unique and razor peptides were used for protein quantification.

Serum drug concentration measurement. The method was described in detail in our earlier publications[9]. The analysis of the drugs was performed using LC-MS/MS system consisting of Shimadzu Nexera X2 HPLC with an AB/Sciex Triple Quad 4500 Q-Trap™ mass spectrometer. The separation was achieved using a C_{18} analytical column (Alltima™, 2.1 X 100 mm, 3 µm) protected by a C_{18} guard column (Phenomenex™ 4.6mm ID cartridge with holder). Various parameters are provided in the table below.

	UT-143
Run time (min)	3.0
Injection volume (µl)	10
Mobile phase	
Channel A	95% acetonitrile + 5% water
Channel B	95% water + 5% acetonitrile

A: B (%)	5:95
Mode	Negative
Declustering Potential (DP)	-125
Collision Energy (CE)	-26
Cell Exit Potential (CXP)	-5
Q1/Q3	461.0/231.6

Medicinal chemistry:

Scheme 1. Synthesis of UT-215[a]

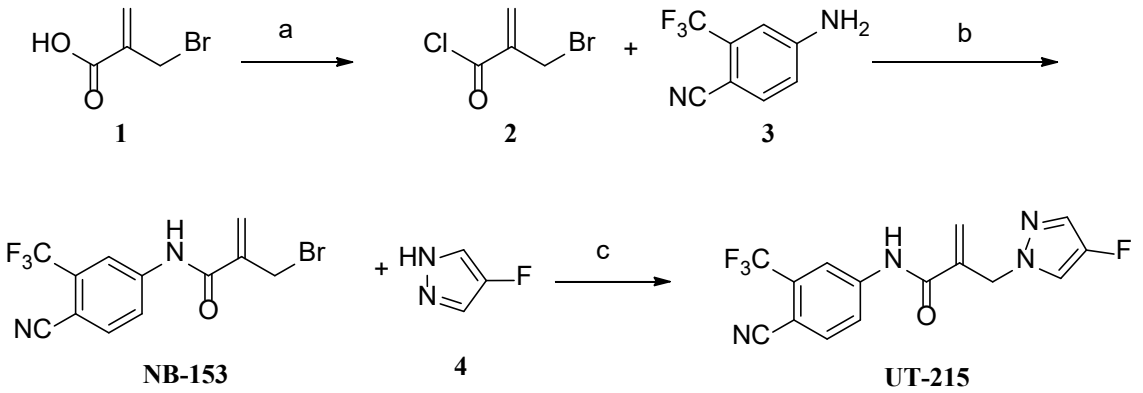

[a] Reagents and conditions:(a) $SOCl_2$ in tetrahydrofuran (THF), -10 to 0 °C; (b) Et_3N in THF, -10 to 0 °C, and then to 50 °C, 2-3 h; (c) NaH in THF, 0 °C to room temperature.

2-(Bromomethyl)-*N*-(4-cyano-3-(trifluoromethyl)phenyl)acrylamide (**NB-153**).

To a solution of 2-(bromomethyl)acrylic acid (**1**, 3.00 g, 18 mmol) in anhydrous THF (30 mL), which was cooled in an ice bath under as argon atmosphere, was added dropwise thionyl chloride (2.60 g, 22 mmol). The reaction mixture was stirred for 1.5 hour. The reaction was cooled to 0-5 ºC. Triethylamine (2.39 g, 24 mmol) was slowly added to the reaction mixture over 10 minutes while maintaining the reaction temperature below 12 ºC. 4-Amino-2-(trifluoromethyl)benzonitrile (**3**, 3.38 g, 18 mmol) was then charged to the batch. The reaction mixture was stirred for 12 hours at room temperature under argon. The product was purified by a silica gel column using DCM and ethyl acetate (19:1; v/v) as eluent to afford 5.16 g (84%) of the titled compound as light brown solid.

^{1}H NMR (400MHz, $CDCl_3$) δ 8.36 (s, 1H, NH), 8.10 (s, 1H, ArH), 8.02-8.00 (m, 1H, ArH), 7.83-7.80 (m, 1H, ArH), 6.11 (s, 1H, C=CH), 5.96 (s, 1H, C=CH), 4.41 (s, 2H, CH_2); Mass (ESI, Positive): 333.04 $[M + H]^+$.

N-(4-Cyano-3-(trifluoromethyl)phenyl)-2-((4-fluoro-1*H*-pyrazol-1-yl)methyl)acrylamide (**UT-215**).

To a solution of 4-fluoro-1*H*-pyrazole (**4**, 0.41 g, 4.8 mmol) in anhydrous THF (20 mL), which was cooled in an ice water bath under an argon atmosphere, was added sodium hydride (60% dispersion in oil, 0.58 g, 14 mmol). After addition, the resulting mixture was stirred for three hours. 2-(Bromomethyl)-*N*-(4-cyano-3-(trifluoromethyl)phenyl)acrylamide (**NB-153**, 1.60 g, 4.8 mmol) was added to above solution, and the resulting reaction mixture was allowed to stir overnight at room temperature under argon. The reaction was quenched by water, extracted with ethyl acetate.

The organic layer was washed with brine, dried with $MgSO_4$, filtered, and concentrated under vacuum. The product was purified by a silica gel column using DCM and ethyl acetate (9:1, v/v) as eluent to afford 0.10 g (6%) of the titled compound (**UT-215**) as white solid.

^{1}H NMR (400MHz, DMSO-d_6) δ 10.80 (s, 1H, N*H*), 8.34 (s, 1H, Ar*H*), 8.14-8.13 (m, 2H, Ar*H*), 7.91-7.90 (m, 1H, Pyrazole-*H*), 7.52-7.51 (m, 1H, Pyrazole-*H*), 6.15 (s, 1H, C=C*H*), 5.59 (s, 1H, C=C*H*), 4.49 (s, 2H, CH_2); HRMS [$C_{15}H_{11}F_4N_4O^+$]: calcd 339.0869, found 339.0892 [M + H] $^+$. Purity: 97.18% (HPLC).

Scheme 2. Synthesis of UT-143[a]

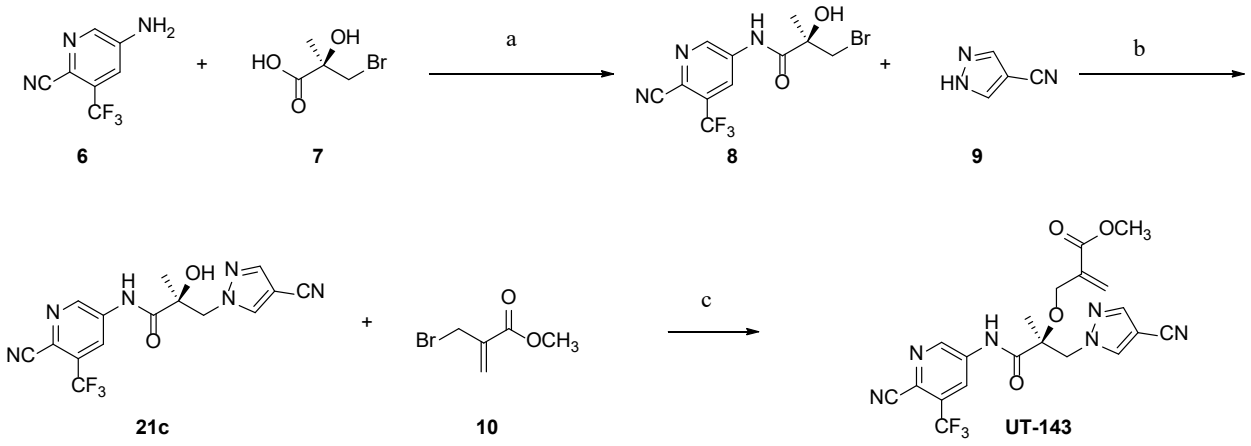

[a] Reagents and conditions:(a) i. $SOCl_2$ in tetrahydrofuran (THF), -10 to 0 °C; ii. Et_3N in THF, -10 to 0 °C, and then to 50 °C, 2-3 h; (c) NaH in THF, 0 °C to room temperature.

(*R*)-3-Bromo-*N*-(6-cyano-5-(trifluoromethyl)pyridin-3-yl)-2-hydroxy-2-methylpropanamide (**8**)

Thionyl chloride (8 mL, 10.7 mol) was added dropwise to a cooled solution (less than 4 ºC) of (*R*)-3-bromo-2-hydroxy-2-methylpropanoic acid (**7**, 1.27 g, 6.94 mmol) in 30 mL of THF under an argon atmosphere. The resulting mixture was stirred for 3 h under the same condition. To this was added Et_3N (18 mL, 12.8 mmol) and stirred for 20 min under the same condition. After 20 min, 5-amino-3-(trifluoromethyl)picolinonitrile (**6**, 1 g, 5.34 mmol), 30 mL of THF were added and then the mixture was allowed to stir overnight at room temperature. The solvent was removed under reduced pressure to give a solid which was treated with 20 mL of H_2O, extracted with EtOAc (2 X 20 mL). The combined organic extracts were washed with saturated $NaHCO_3$ solution (2 X 10 mL) and brine (30 mL). The organic layer was dried over anhydrous $MgSO_4$ and concentrated under reduced pressure to give a solid which was purified from column chromatography using CH_2Cl_2/EtOAc (4:1, v/v) to give a solid. This solid was recrystallized from CH_2Cl_2/hexane to give 1.32 g (70.2%) of (*R*)-3-bromo-*N*-(6-cyano-5-(trifluoromethyl)pyridin-3-yl)-2-hydroxy-2-methylpropanamide (**3**) as a light-yellow solid. MS (ESI) *m/z* 351.08 $[M - H]^-$.^{1}H NMR ($CDCl_3$, 400 MHz) δ 9.15 (bs, 1H, N*H*), 8.90 (s, 1H), 8.78 (s, 1H), 4.02 (d, *J* = 10.8 Hz, 1H), 3.60 (d, *J* = 10.8 Hz, 1H), 3.17 (bs, 1H, O*H*), 1.66 (s, 3H).; ^{19}F NMR ($CDCl_3$, 400 MHz) δ -62.09.

(*S*)-3-(4-Cyano-1*H*-pyrazol-1-yl)-*N*-(6-cyano-5-(trifluoromethyl)pyridin-3-yl)-2-hydroxy-2-methylpropanamide (**21c**)

To a dry, nitrogen-purged 50 mL round-bottom flask equipped a dropping funnel under argon atmosphere, NaH of 60% dispersion in mineral oil (511 mg, 12.8 mmol) was added in 5 mL of anhydrous THF solvent in the flask at ice-water bath, and 1*H*-pyrazole-4-carbonitrile (**9**, 465 mg,

4.26 mmol) was stirred 30 min at the ice-water bath. Into the flask, compound **8** (1.5g, 4.26 mmol) in 5 mL of anhydrous THF was added through dropping funnel under argon atmosphere at the ice-water bath and stirred overnight at room temperature. After adding 1 mL of H_2O, the reaction mixture was condensed under reduced pressure, and then dispersed into 50 mL of EtOAc, washed with 50 mL (x 2) water, evaporated, dried over anhydrous $MgSO_4$, and evaporated to dryness. The mixture was purified with flash column chromatography as an eluent EtOAc/ Hexane = 1/1 to produce targeted **21c** as white solid (total 52% yield). MP 169.7-169.9 ºC; UV max 195.45, 274.45; MS (ESI) *m/z* 363.1 $[M - H]^-$; 365.0 $[M + H]^+$; HRMS (ESI) *m/z* calcd for $C_{15}H_{11}F_3N_6O_2$ 365.0974 $[M + H]^+$ found 365.0968 $[M + H]^+$; 387.0790 $[M + Na]^+$; Purity (LC, t_{min} 2.97) 97.28%; ^1H NMR ($CDCl_3$, 400 MHz) d 9.17 (bs, 1H, N*H*), 8.83 (s, 1H), 8.67 (d, *J* = 1.6 Hz, 1H),, 7.92 (s, 1H), 7.85 (s, 1H), 5.58 (s, OH), 4.73 (d, *J* = 14.0 Hz, 1H), 4.34 (d, *J* = 14.0 Hz, 1H), 1.53 (s, 3H); ^{19}F NMR ($CDCl_3$, 400 MHz) d -62.11.

(*S*)-Methyl 2-(((3-(4-cyano-1*H*-pyrazol-1-yl)-1-((6-cyano-5-(trifluoromethyl)pyridin-3-yl)amino)-2-methyl-1-oxopropan-2-yl)oxy)methyl)acrylate (**UT-143**)

To a dry, nitrogen-purged 50 mL round-bottom flask equipped a dropping funnel under argon atmosphere, NaH of 60% dispersion in mineral oil (44 mg, 1.1 mmol) was added in 5 mL of anhydrous THF solvent in the flask at ice-water bath, and 1*H*-pyrazole-4-carbonitrile (**9**, 465 mg, 4.26 mmol) was stirred 30 min at the ice-water bath. To the solution, a solution of methyl 2-(bromomethyl)acrylate (0.2 mL, 0.74 mmol) in 5 mL of THF was added dropwise to a stirred solution of a solution of compound **21c** (200 mg, 0.54 mmol) in anhydrous THF (10 mL) over 10 min at room temperature. The solution was then stirred at room temperature. The solution was then stirred overnight at room temperature and the solution concentrated in vacuo. The residue was then taken up in water and extracted four times with ethyl acetate. The combined ethyl acetate solution

was washed with saturated sodium chloride, dried over anhydrous magnesium sulfate, filtered, and concentrated. The residue was then purified by silica gel column chromatography eluting with hexane/ethyl acetate 1:1 (v/v), to give desired product as a white solid (**UT-143**, yield 38%) and (*S*)-methyl 2-((3-(4-cyano-1*H*-pyrazol-1-yl)-*N*-(6-cyano-5-(trifluoromethyl)pyridin-3-yl)-2-hydroxy-2-methylpropanamido)methyl)acrylate (yield 25%).

MS (ESI) *m/z* 461.23 $[M - H]^-$; 463.27 $[M + H]^+$; 485.21 $[M + Na]^+$; HRMS (ESI) *m/z* calcd for $C_{20}H_{17}F_3N_6O_4$ 463.1342 $[M + H]^+$ found 463.1342 $[M + H]^+$; ^{1}H NMR ($CDCl_3$, 400 MHz) d 10.61 (bs, 1H, N*H*-C(O)), 9.17 (s, 1H), 8.89 (s, 1H), 7.85 (s, 1H), 7.72 (s, 1H), 6.52 (s, 1H), 6.08 (s, 1H), 4.55 (d, *J* = 13.6 Hz, 1H), 4.41 (d, *J* = 13.6 Hz, 1H), 4.36 (d, *J* = 9.2 Hz, 1H), 4.09 (d, *J* = 9.2 Hz, 1H), 3.77 (s, 3H, O-C*H*$_3$), 1.59 (s, 3H, CH_3); ^{13}C NMR ($CDCl_3$, 100 MHz) d 171.61, 167.86, 144.47, 142.90, 142.00, 137.52, 136.30, 132.23, 131.14 (q, *J* = 33.5 Hz), 125.00, 123.87 (d, *J* = 4.8 Hz), 123.02, 120.29, 114.42, 113.13, 92.78, 80.96, 65.63, 59.73, 53.11, 18.27; ^{19}F NMR ($CDCl_3$, 400 MHz) d -62.15.

References

1. Mohammed, H.; Taylor, C.; Brown, G. D.; Papachristou, E. K.; Carroll, J. S.; D'Santos, C. S., Rapid immunoprecipitation mass spectrometry of endogenous proteins (RIME) for analysis of chromatin complexes. *Nat Protoc* **2016,** *11* (2), 316-26.

2. Papachristou, E. K.; Kishore, K.; Holding, A. N.; Harvey, K.; Roumeliotis, T. I.; Chilamakuri, C. S. R.; Omarjee, S.; Chia, K. M.; Swarbrick, A.; Lim, E.; Markowetz, F.; Eldridge, M.; Siersbaek, R.; D'Santos, C. S.; Carroll, J. S., A quantitative mass spectrometry-based approach to monitor the dynamics of endogenous chromatin-associated protein complexes. *Nat Commun* **2018,** *9* (1), 2311.
3. Ritchie, M. E.; Phipson, B.; Wu, D.; Hu, Y.; Law, C. W.; Shi, W.; Smyth, G. K., limma powers differential expression analyses for RNA-sequencing and microarray studies. *Nucleic Acids Res* **2015,** *43* (7), e47.
4. Hochberg, Y.; Benjamini, Y., More powerful procedures for multiple significance testing. *Stat Med* **1990,** *9* (7), 811-8.
5. Szklarczyk, D.; Gable, A. L.; Nastou, K. C.; Lyon, D.; Kirsch, R.; Pyysalo, S.; Doncheva, N. T.; Legeay, M.; Fang, T.; Bork, P.; Jensen, L. J.; von Mering, C., The STRING database in 2021: customizable protein-protein networks, and functional characterization of user-uploaded gene/measurement sets. *Nucleic Acids Res* **2021,** *49* (D1), D605-D612.
6. Corces, M. R.; Trevino, A. E.; Hamilton, E. G.; Greenside, P. G.; Sinnott-Armstrong, N. A.; Vesuna, S.; Satpathy, A. T.; Rubin, A. J.; Montine, K. S.; Wu, B.; Kathiria, A.; Cho, S. W.; Mumbach, M. R.; Carter, A. C.; Kasowski, M.; Orloff, L. A.; Risca, V. I.; Kundaje, A.; Khavari, P. A.; Montine, T. J.; Greenleaf, W. J.; Chang, H. Y., An improved ATAC-seq protocol reduces background and enables interrogation of frozen tissues. *Nat Methods* **2017,** *14* (10), 959-962.
7. Bohl, C. E.; Gao, W.; Miller, D. D.; Bell, C. E.; Dalton, J. T., Structural basis for antagonism and resistance of bicalutamide in prostate cancer. *Proceedings of the National Academy of Sciences of the United States of America* **2005,** *102* (17), 6201-6.
8. Bohl, C. E.; Miller, D. D.; Chen, J.; Bell, C. E.; Dalton, J. T., Structural basis for accommodation of nonsteroidal ligands in the androgen receptor. *The Journal of biological chemistry* **2005,** *280* (45), 37747-54.
9. Ponnusamy, S.; He, Y.; Hwang, D. J.; Thiyagarajan, T.; Houtman, R.; Bocharova, V.; Sumpter, B. G.; Fernandez, E.; Johnson, D. L.; Du, Z.; Pfeffer, L. M.; Getzenberg, R. H.; McEwan, I. J.; Miller, D. D.; Narayanan, R., Orally-Bioavailable Androgen Receptor Degrader, A Potential Next-Generation Therapeutic for Enzalutamide-Resistant Prostate Cancer. *Clin Cancer Res* **2019**.